6th European Conference on Computational Mechanics (ECCM 6)
7th European Conference on Computational Fluid Dynamics (ECFD 7)
1115 June 2018, Glasgow, UK

EIGENMODE OPTIMIZATION OF A CONTRACTION CHANNEL BASED ON STABILITY ANALYSIS

Yinzhu Wang[1,3], Alejandro Martínez-Cava[1], Eusebio Valero[1,2], Yao Zheng[3] AND Esteban Ferrer[1,2]

[1] ETSIAE-UPM - Universidad Politécnica de Madrid
Plaza de Cardenal Cisneros 3, 28040 Madrid, Spain

[2] CCS-UPM - Centre for Computational Simulation
Universidad Politécnica de Madrid, Boadilla del Monte, 28660 Madrid, Spain

[3] CESC-ZJU - Centre for Engineering and Scientific Computation
Zhejiang University, Hangzhou, Zhejiang 310027, P.R. China

Key words: Geometric Optimisation, Eigenvalue Problem, Contraction Channel, Linear Stability Analysis

Abstract. This work studies flow control in a channel flow with a sudden geometry contraction. Optimization investigations have been carried out aiming at minimizing the amplification rate of the most unstable mode, to keep the symmetric flow topology in the contraction channel. In this framework, the DLR-TAU code is employed to obtain the compressible base flow solution, from which the critical Reynolds numbers for the bifurcations have been found. A first-discretize-then-linearize approach was used, taking advantage of the linear Jacobian matrix implementation present in the DLR-TAU code for stability analysis, from which the eigenmodes responsible for the bifurcations are obtained.

A geometry parametrized representation, an FFD mesh deformation program and a dynamically updated RBF surrogate model are developed to drive the optimization investigation. In this investigation, geometry configurations with negative amplification rates have been obtained, making the eigenmodes stable. The potential of the method is illustrated by the increase of critical Reynolds number of bifurcation.

1 INTRODUCTION

There are many applications in which the flow meets a sudden geometry contraction, for example, the cooling flow in a turbine blade. Evidence has shown that the contraction in the cooling flow in a turbine blade may cause some unfavourable pressure perturbations downstream, affecting the next blades, therefore causing fatigue and loss of efficiency [1].

There have been several investigations aiming at understanding the flow behaviour in sudden contractions both numerically and experimentally. In numerical simulations carried out by Chiang and Sheu [2], and experimental investigations carried out by Cherdron and Soby [3], two recirculation bubbles of different sizes were observed on the two tip

corners downstream the contraction stage. Chiang and Sheu's numerical investigation shows that above a certain critical Reynolds number, the flow appears to be no longer symmetric about the centre line of the channel, in which a pitchfork bifurcation is found to occur.

This non-symmetrical flow topology can be analysed using global stability analysis, evaluating the influence of the Reynolds number of the flow as the main parameter that triggers the unstable phenomenon [4]. A previous work was carried out over a coolant channel on the trailing edge of a turbine blade [5], identifying the strong correlations between the plenum and channel areas and the base region. In the current work, the eigenmode that is responsible for the non-symmetrical flow topology is analysed.

In recent years, aerodynamic optimization has been an active field of research and is becoming a common practice in aerospace engineering. The advances in computing power and development of more accurate computational fluid dynamics codes have been promoting optimal shape design for particular applications specified by constraints on geometry load [6]. However, design optimization investigations have been scarcely seen in the field of stability analysis. It may be worthwhile to work on sophisticated methods based on surrogate models in order to perform design optimization and design space approximation at an affordable computational cost.

In this paper, optimization investigation on minimizing the amplification rate of the asymmetric mode is carried out, which, to the authors' knowledge, has not been done before.

The remaining sections of this paper are organized as follows. In section 2, the mathematical models and numerical procedures with which we work is presented. This is followed by compressible bifurcation study, stability analysis on the contraction channels of different contraction ratios and of different Reynolds numbers, and an optimization loop for the optimization investigations. Finally, in section 4, concluding remarks are provided.

2 Bifurcation study

2.1 Methodology

2.1.1 CFD Model

In this paper we utilize a compressible version of the laminar Navier-Stocks equations. The set of equations, written in conservative form, can be expressed as:

$$\frac{\partial}{\partial t}\iiint_V \boldsymbol{Q} dV = -\iint_S \boldsymbol{F}\cdot\boldsymbol{n} dS \tag{1}$$

and the flux density tensor $\boldsymbol{F}$ can be decomposed along the three Cartesian coordinate directions and comprises the inviscid, viscous and turbulent fluxes. The flow is considered as ideal gas, where the heat capacities at constant pressure and volume are assumed constant. The NS equations are discretized using a finite volume approach, where hexahedrals were used to generate an anisotropic three-dimensional mesh, with only one span-wise cell to

be reduced to a two-dimensional mesh during a mesh-preprocessing step. The boundary conditions imposed on the body surface were

$$u = v = w = 0, \qquad \hat{\nu} = 0, \qquad \frac{\partial T}{\partial \boldsymbol{n}} = \frac{\partial \rho}{\partial \boldsymbol{n}} = 0, \tag{2}$$

where $\boldsymbol{n}$ is the normal direction to the body surface. Inflow boundary conditions were imposed at the inflow region of the domain, whereas pressure-outflow conditions were used. Viscous wall boundary conditions were used for the upper and lower boundaries.

For the stable (symmetrical) configurations. Base flow solutions were obtained using the DLR-TAU code solver, employing a second order Van Leer Upwind scheme for the convective and turbulence terms until convergence was achieved. The convergence criteria, set up to values lower than 10^{-5}, was evaluated through the global density residual, being this defined as:

$$\|res_\rho^n\| = \sqrt{\sum_{j=1}^{N_P} \frac{[res_\rho^n(j)]^2}{N_P}}, \tag{3}$$

where N_P denotes the number of grid points.

For the unstable (non-symmetrical) configurations, an unsteady approach was used, restarting from a non-converged steady RANS solution. The timestep and number of inner iterations were evaluated to ensure convergence on each timestep, keeping the global residual value always below 10^{-6}.

2.1.2 Stability Analysis

On the resolution of the linearized stability analysis of the flow solution, a first-discretize-then-linearize approach was used, taking advantage of the linear Jacobian matrix implementation present on the DLR-TAU code [7]. From equation (1), the finite volume formulation can be written in compact form as:

$$\boldsymbol{B}\frac{\partial \boldsymbol{Q}}{\partial t} = \boldsymbol{R}(\boldsymbol{Q}), \tag{4}$$

where $\mathbf{B}$ is a diagonal matrix with leading dimension $N_b N$ containing the volumes associated to each finite cell, N being the number of finite volumes contained in the domain, and $\mathbf{R}$ is the residual, equivalent to the flux contributions. BiGlobal stability analysis considers a two-dimensional flow (two non-homogeneous directions $x-z$) plus a spanwise periodic component y, namely treated as:

$$\boldsymbol{U}(x,y,z) = \bar{\boldsymbol{U}}(x,z) + \epsilon \hat{\boldsymbol{U}}(x,z)e^{i(\beta y - \sigma t)}, \tag{5}$$

where $\sigma = \sigma_R + i\sigma_I$ is the complex eigenvalue, $\bar{\boldsymbol{U}}$ is a particular solution of the steady RANS problem (i.e. $\boldsymbol{R}(\bar{\boldsymbol{U}}) = 0$) and $\hat{\boldsymbol{U}}$ describes the complex eigenmode. For this problem, the spanwise wavenumber β has been considered constant and equal to zero, assuming a purely 2D configuration. With these assumptions, the purely real generalized eigenvalue problem for the determination of ω remains as:

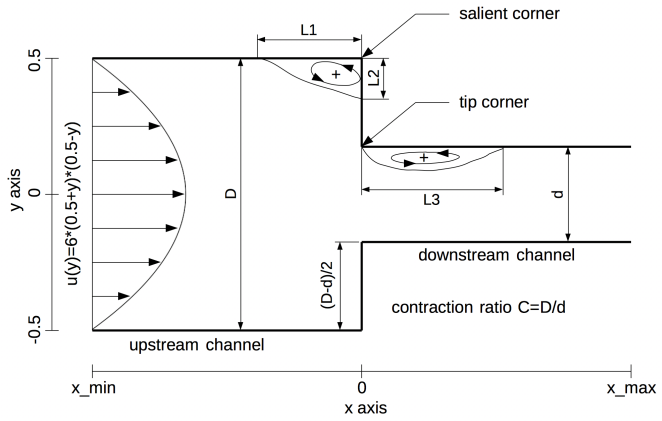

Figure 1: Geometry and the lengths chosen to characterize the flow features

$$\left[\frac{\partial \boldsymbol{R}}{\partial \boldsymbol{U}}\right]_{\bar{\boldsymbol{U}}} \hat{\boldsymbol{U}} = \sigma \boldsymbol{B} \hat{\boldsymbol{U}}, \tag{6}$$

which can also be expressed as:

$$\boldsymbol{A} \hat{\boldsymbol{U}} = \sigma \boldsymbol{B} \hat{\boldsymbol{U}}, \tag{7}$$

where the matrix $\boldsymbol{A} = \left[\frac{\partial \boldsymbol{R}}{\partial \boldsymbol{U}}\right]_{\bar{\boldsymbol{U}}}$ is the Jacobian of the system, which can be computed once the steady base flow has converged.

A full LU factorization is performed for the Jacobian matrix **A** using the MUMPS package [8], followed by a Arnoldy algorithm with shift-and-invert transformation to finally obtain the eigenvalues of a reduced Krylov subspace throughout LAPACK [9] routines.

2.2 Numerical results

2.2.1 CFD simulation

In this current investigation, both full and half domains of a 2-D contraction channel are taken into account for comparison. As shown in figure 1, D and d are the widths of the channels upstream and downstream the contraction, respectively. $(0 - x_{min})$ and $(x_{max} - 0)$ are the lengths of the two channels. L_1 is the separation length of the salient corner bubble, L_2, L_3 are the reattachment lengths of the salient corner bubble and the tip corner bubble respectively, which are defined as the x-axis distance between the separation point and the reattachment point on the walls shown in figure 1.

The upstream Reynolds number is characterized as $Re = \rho V D/\mu$, where V is the mean velocity of the upstream flow, and ρ, μ are the density and dynamic viscosity. Dirichlet boundary conditions are imposed at the inlets with a velocity profile $V(y) = 6 * (0.5 + y) * (0.5 - y)$, as a fully developed velocity profile. The outlets are considered as pressure exits. The walls are considered as viscous walls. Particularly, a symmetric plane is introduced into the half domain geometry.

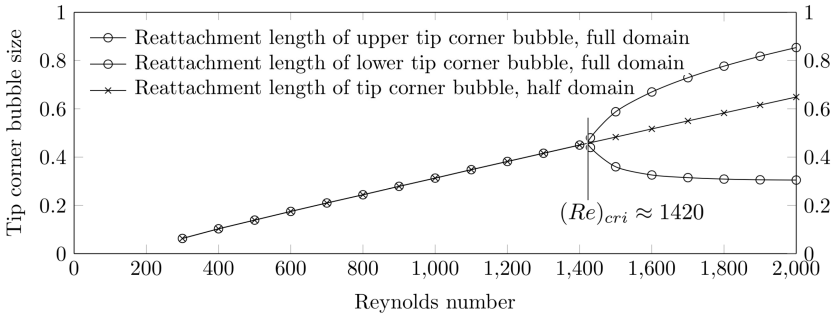

Figure 2: Reattachment lengths L_3 of downstream tip corner eddy against Reynolds numbers, $C = 4$

(a) $Re1000$ (b) $Re2000$

Figure 3: U_x for $Re1000$ and $Re2000$, $C = 4$, full domain

In the present investigation, flows through three contraction channels with different contraction ratios were simulated to study the bifurcations. We took L_3 as the judgement of the bifurcations. For contraction ratio $C = 2, 4, 8$, we simulate both half and full domains, and the critical Reynolds numbers for the pitchfork bifurcations are obtained. We simulated from Reynolds number 500 to 4000, 800 to 2000 and 800 to 2000, and got the critical Reynolds numbers, which are 3150, 1420 and 1230, respectively. More detailed data of L_3 against Reynolds number are shown in figure 2. We can see that the differences of reattachment lengths of the two recirculation bubbles get larger with the Reynolds number increasing.

Specifically, we present the results at Reynolds number 1000 and 2000 for contraction ratio $C = 4$, shown in figure 3. As the recirculation bubbles at the tip corners grow in size, the flow channel with a positive v_x becomes smaller, making the two bubbles closer to each other, and easier for the two to have momentum transfer between one and another.

The mechanism of how a flow develops from symmetric to asymmetric configuration in a symmetric channel has been an important academic subject for many years. Hawa and Rusak [10] presented that the instability resulted from interaction between the destabilizing upstream convection effects by the asymmetric perturbation and the combined stabilizing effects of the viscous dissipation and the downstream convection of perturbations by the base symmetric flow. Chiang and Sheu [2] believed that the observed

(a) $Re1000$ (b) $Re2000$

Figure 4: Eigenvalue spectrums for $Re1000$ and $Re2000$, $C = 4$

(a) u_x, $Re1000$ (b) u_x, $Re2000$

Figure 5: Eigenvectors of direct modes for $Re1000$ and $Re2000$

asymmetric disturbance originates from imperfections, such as any sort of asymmetry in the channel geometry and the incoming flow conditions in the experiments, and limited finite precision in numerical computation known as the machine round-off error. In the next section, we will try to explain this mechanism in a stability aspect of view.

2.2.2 Stability analysis

We conducted stability analysis for Reynolds number ranges 2500 to 4000, 900 to 2000, 900 to 2000, for contraction ratios 2, 4 and 8, respectively.

As an example, we present the results of Reynolds number 1000 and 2000 for contraction ratio $C = 4$. figure 4a and figure 4b demonstrate the eigenvalue spectrum for Reynolds number 1000 and 2000, respectively. We can see in the eigenvalue spectrum for Reynolds number 2000, that there is one eigenvalue which has a real part that is larger than 0. And the corresponding eigenvector is shown in figure 5b. This eigenvalue has a imaginary part which is equal to 0, and a real part which is larger than 0, which indicates the temporal frequency of it is corresponding eigenmode is 0, and the amplification rate of this mode is larger than 0, making this mode unstable. Additionally, we observe the mode is not symmetric. This mode is therefore responsible for the first bifurcation. Using a mode tracking scheme, which will be explained in section 3.2, we identified this mode for Reynolds number 1000, which is shown in figure 5a.

When the amplification rate is below zero, the mode does not grow. Meanwhile, with a

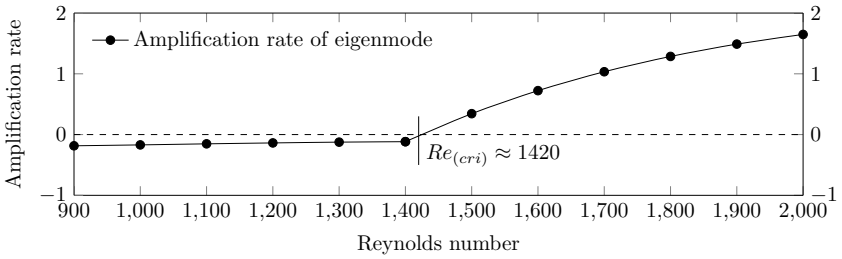

Figure 6: Amplification rates against Reynolds number, $C = 4$

positive amplification rate, the mode amplifies over time, and eventually to the magnitude of the base flow, causing the unstable flow features.

In figure 6, we present the chart of amplification rates against the Reynolds numbers. By compare them to the bifurcation charts in section 3.1, we can determine that the bifurcations start at the exact same Reynolds numbers for the 3 different contraction ratios.

3 Optimization

Bearing in mind that real part of the eigenvalue stands for the amplification rate of the corresponding eigenmode, the optimization problem can be simplified as minimizing the real part of the corresponding eigenvalue of a specific eigenmode of interest. Based on this assumption, the optimization problem is modelled as follows.

$$\begin{aligned} &min_{d\in D} \quad \boldsymbol{g}(\boldsymbol{d},\boldsymbol{\theta}) \\ &subject \quad to: \quad h_i(\boldsymbol{d},\boldsymbol{\theta}) >= 0, \quad for \quad i = 1, \quad ..., \quad N \end{aligned} \tag{8}$$

in which, $\boldsymbol{d}$ is the geometry parameters and $\boldsymbol{\theta}$ is the model parameters in the flow field.

The objective function $g(\boldsymbol{d},\boldsymbol{\theta}) = \omega_r(\boldsymbol{d},\boldsymbol{\theta})$, which is dependent on the geometry parameters $\boldsymbol{d}$ and the model parameters $\boldsymbol{\theta}$ are minimized over all possible designs, subjected to constraints imposed on both geometry and the flow field. The flow chart of the optimization is shown in figure 7.

3.1 Methodology

3.1.1 Genetic Algorithm

The genetic algorithm is a computational model that emulates the process of natural selection and genetic mechanism in Darwin's evolutionary, and seeks the optimal solution through a natural genetic process [11]. It is suitable for solving both constrained and unconstrained optimization problems. The genetic algorithm starts with an initial population (a set of potential solutions), which is consisted of a number of individuals with combinations of different genes. A gene is a member in a parameter array of an individual. Starting with the initial population, by calling cost function, the fitness of each individual is evaluated, through which the best individuals are selected. After the process of crossover and mutation, a new generation is obtained. In this process, a new

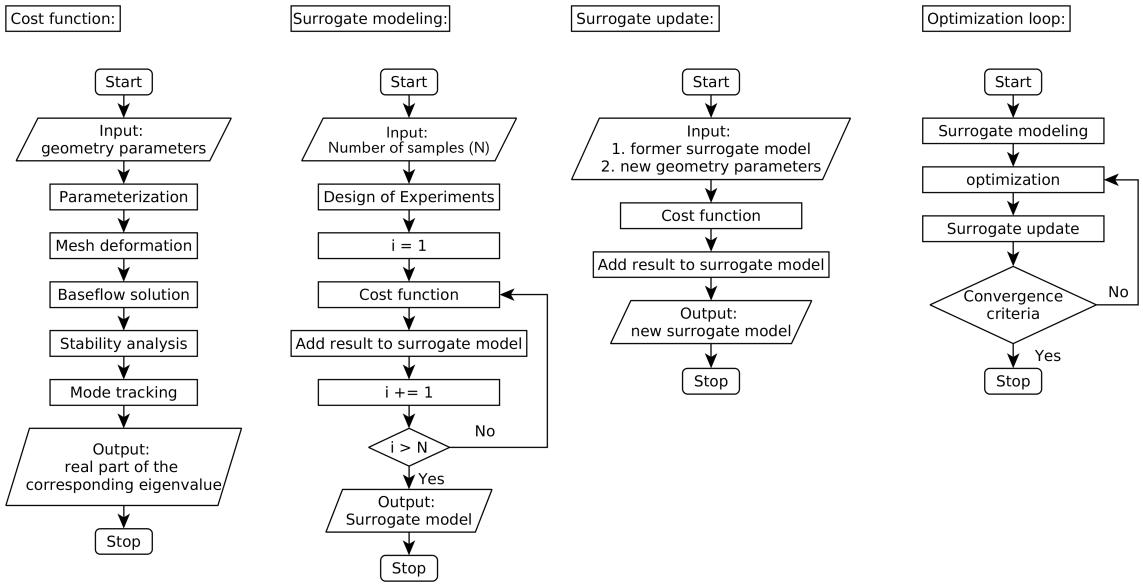

Figure 7: The optimization loop

generation always has higher fitness than the former. After a certain amount of iterations, an optimal solution is obtained.

3.1.2 Radial Bases Funciton

RBF (Radial Basis Function) interpolation is a popular method for constructing surrogates suitable for highly non-linear data using irregular distributions of sample points, which can be adapted to the function being modelled.

A Radial Basis Function (RBF) method is a linear combination of a series of basis functions, whose argument is the Euclidean distance between the interpolation point x and all the other points in the known data set. The model has the form

$$f(x) = \sum_{i=1}^{N} w_i \phi ||x - x_i||, \tag{9}$$

where x is the interpolation point, ϕ is the chosen basis function, w_i is the weight coefficient for each basis function, and $|| * ||$ represents the Euclidean norm. Any function ϕ that satisfies the property of $\phi(x) = \phi(||x||)$ is a radial function, and can be used as a basis function in RBFs.

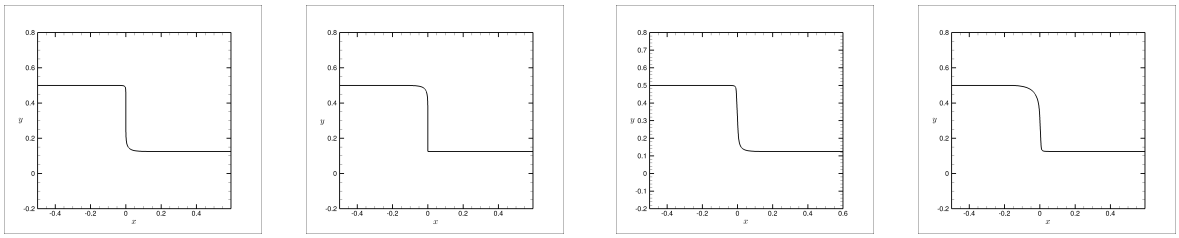

Figure 8: Examples of the parametrization

3.1.3 Parametrization

For this optimization investigation, a special geometry parametrization method based on super-elliptic curve is developed. The equation has the form:

$$\left|\frac{x}{a}\right|^n + \left|\frac{y}{b}\right|^n = 1 \tag{10}$$

In this context, $a = b$ as it is favourable for the major and minor axis of the super-ellipse to be equal to each other, for reducing the number of the geometry parameters for less computational cost. With higher degree, the curvature radius gets smaller. This parametrization method provides continuous curvature at the intersection point between the parametrized part and the rest of the geometry, making the transition of the geometry more smooth.

As shown in figure 5, the mode of interest and the most unstable modes are located near the salient corner and the tip corner, so the target of this parametrization is to reshape the parts of the boundary near this region. The salient corner and the top corner are parametrized as two sections of super-elliptic curves. The degree of the super-elliptic curve controls the largest curvature of the curve which is located near the tip. Another parameter is added to control the tangential direction of the contraction stage with respect to the vertical direction. Some examples of this parametrization method are shown in the figure 8.

3.1.4 Mode Tracking

The optimization investigation is coupled with stability analysis, and it is necessary to avoid manual work on eigenvector matching for identifying the eigenmodes and eigenvalues of interest. A Modal Assurance Criterion (MAC) was developed and successfully used by Nobari et al. [12], which has the form:

$$MAC(\mathbf{\Phi_1}, \mathbf{\Phi_2}) = \left(\frac{\left|\mathbf{\Phi_1^*} \quad \mathbf{\Phi_2}\right|}{||\mathbf{\Phi_1}|| \quad ||\mathbf{\Phi_2}||}\right)^2, \tag{11}$$

3.2 Optimization results

In the current optimization investigation, we aim at Reynolds numbers 3200, 1500 and 1300 for $C = 2, 4, 8$ respectively. For testing the change of amplification rate by a small amount of deformation on the boundary.

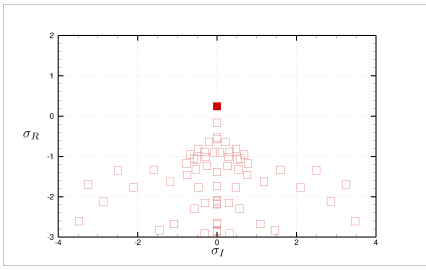

(a) Original eigenvalue spectrum

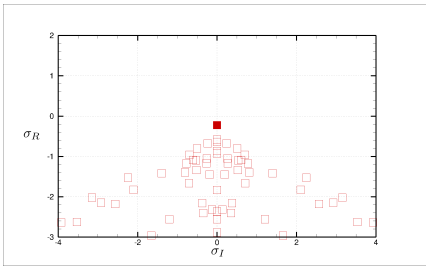

(b) Optimized eigenvalue spectrum

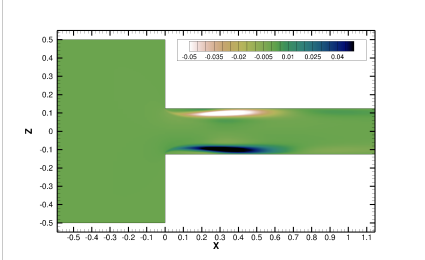

(c) Original eigenvector

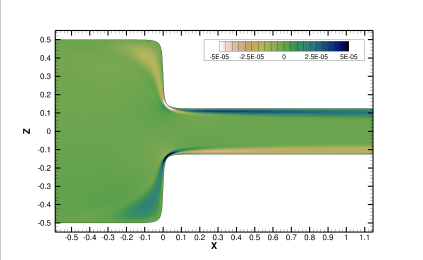

(d) Opimized eigenvector

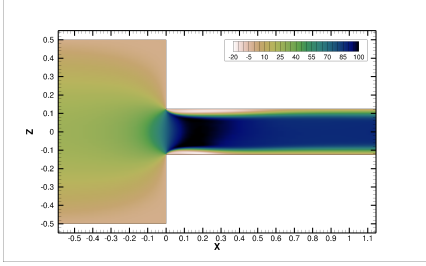

(e) Original velocity contour

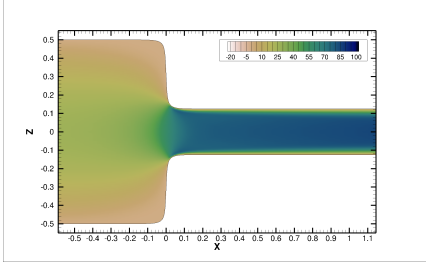

(f) Optimized velocity contour

Figure 9: Comparison between original and optimized geometry configurations, $C = 4$

The result of optimization in comparison with the original results are shown in figure 9. For the three contraction ratios, in comparison with the original geometry configurations, we can find that the tip and salient corners are rounded and the contraction stages are also tilted. The optimal configurations reach the edge of the design space, which means if the design space is enlarged, the optimal configurations may go beyond the current design space. However, as is discussed before, the design space is narrowly restricted near the original geometry configuration due to the linearity in stability analysis.

We can see in the eigenvalue spectrum shown in figure 9b in comparison with figure 9a that the amplification rates of the most unstable asymmetric modes for each contraction ratio are reduced and below zero after the optimization. The corresponding eigenvectors are shown in figure 9d in comparison with figure 9c, from which we can find that the modes have been relocated from behind the tip corners to around the corner. The new modes lie along the boundaries before and after the tip corners.

We conducted simulations with full domains for the original and optimal geometry

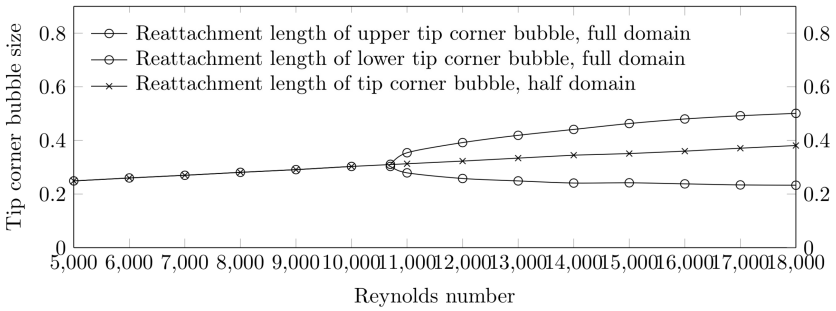

Figure 10: Bifurcation of the optimized and the original geometry configuration, $C = 4$

configurations. The results of the optimization are shown in figure 9f, in comparison with the original results shown in figure 9e. After the optimization, the flows are all symmetric and the sizes of the recirculation bubbles are either reduced greatly.

After the optimal designs are obtained, we carried out the bifurcation study on contraction ratio $C = 2$, with the new optimal geometry configuration to see how far the critical Reynolds numbers of bifurcation could be "pushed forward". The reattachment length against Reynolds number of the new shapes are shown in figure 10. The critical Reynolds numbers of bifurcation are increased to around 10700, proving that the critical Reynolds number of bifurcation can be increased with the optimal geometry configuration obtained with a lower Reynolds number.

4 Conclusions and discussion

- Computational investigations have been performed to study flow bifurcation in the symmetric planar contraction channel, which confirm the presence of the pitchfork bifurcation. The critical Reynolds numbers of bifurcations are obtained.

- Stability analysis on the contraction flow has been carried out. The eigenmodes responsible for the flow bifurcations are identified, and their amplification rates are found.

- An efficient optimization method based on stability analysis is developed for investigations on suppressing the modes responsible for unstable flow, and is successfully applied to suppress the unfavourable modes in channel flows with sudden geometry contraction. In this investigation, the amplification rates are reduced and kept stable. We show that the critical Reynolds number of bifurcation can be "pushed forward" with the optimal geometry configuration obtained with a lower Reynolds number.

5 Acknowledgement

This work is part of the project SSeMID, and has received funding from the European Unions Horizon 2020 research and innovation programme under the Marie Skodowska-Curie grant agreement No. 675008.

REFERENCES

[1] Gorbachova, Y. *Stability of trailing edge flow discharge in supersonic regime*. School of Aeronautical Engineering (UPM), 2015.

[2] Chiang, T. P., and Sheu, T. W. H. Bifurcations of Flow Through Plane Symmetric Channel. *Journal of Fluids Engineering* (2002) **124**: 444-451.

[3] Cherdron, W., Durst, F., and Whitelaw, J. H. Asymmetric flows and instabilities in symmetric ducts with sudden expansions. *Journal of Fluid Mechanics* (1978) **84**: 13.

[4] Iorio, M. C., Gonzlez, L. M., and Ferrer, E. Direct and adjoint global stability analysis of turbulent transonic flows over a NACA0012 profile. *International Journal for Numerical Methods in Fluids* (2014) **76**: 147-168.

[5] Gorbachova, Y., Valero, E., Martinez-Cava, A., Paniagua, G., and Saracoglu, B. H. Study of the attainable flow topologies in a supersonic blunt trailing edge at various blowing ratios. *54th AIAA Aerospace Sciences Meeting* (2016) **110**: 82-102.

[6] Huyse, L., Padula, S. L., Lewis, R. M., and Li, W. Probabilistic approach to free-form airfoil shape optimization under uncertainty *AIAA Journal* (2002) **40**: 1764-1772.

[7] Schwamborn, D., Gerhold, T., and Kessler, R. The DLR-TAU Code - an Overview. *ONERA-DLR Aerospace Symposium ODAS* (1999).

[8] Amestoy, P. R., Duff, I. S., LExcellent, J.-Y., and Koster, J. A Fully Asynchronous Multifrontal Solver Using Distributed Dynamic Scheduling. *SIAM Journal on Matrix Analysis and Applications* (2001) **23**: 15-41.

[9] Planitz, M., and Anderson, E. LAPACK Users Guide. *The Mathematical Gazette* (1995) **79**: 210.

[10] Hawa, T., and Rusak, Z. The dynamics of a laminar flow in a symmetric channel with a sudden expansion. *Journal of Fluid Mechanics* (2001) **436**: 283-320.

[11] Kumar, M., Husian, M., Upreti, N., and Gupta, D. Genetic Algorithm: Review and Application. *International Journal of Information Technology and Knowledge Management* (2010) **2**: 451-454.

[12] Jiang, A.-H., Huang, X.-C., Zhang, Z.-H., Li, J., Zhang, Z.-Y., and Hua, H.-X. Uncertainty quantification of squeal instability via surrogate modelling. *Mechanical Systems and Signal Processing* (2010) **24**: 2947-2960.